How reliable are efficiency measurements of perovskite solar cells? The first inter-comparison, between two accredited and eight non-accredited laboratories

Supporting Information

1. Details on fabrication and packaging of perovskite devices

Fabrication

The perovskite devices were supplied by an external laboratory, the name of which is not disclosed here due to reasons of commercial confidentiality.

Preparation of substrates:

Glass substrates were prepared from fluorine-doped tin oxide (FTO) coated glass (8 Ω□, Pilkington), patterned and then washed sequentially in 1-2 v/v% Hellmanex solution, followed by Milli-Q (18.2 MΩ) water, rinsed with isopropanol and blown dry under a stream of N_2. A dense TiO_2 blocking layer (BL) was deposited by screen-printing (Dyesol BL-1) and calcined at 450 °C for 30 min).
For this study, two device architectures were prepared using metal-free, carbon electrodes with $CH_3NH_3PbI_3$ and a mixed-cation perovskite (5-AVA)x(MA)1-xPbI_3, where 5-AVA = 5-ammoniumvaleric acid, as the active material – type 1, referred to as "fast responding" and type 2, referred to as "slow responding", respectively.

"fast responding cell":

Hole-conductor-free, "fast responding" devices were prepared according to the reported procedure of Huawei Zhou et al.[1] The carbon paste dispersion was prepared as described, sealed and stored under gentle mixing/rolling until further required. Patterned FTO substrates, with blocking layers, were coated with a mesoporous TiO_2 layer (Dyesol 18NRT), diluted with ethanol, screen printed and calcined at 500 °C for 30 min prior to treatment via a two-step sequential deposition process, as reported by Burschka et al.[2] The carbon electrode was blade-coated using the paste as prepared above, followed by drying at 70 °C for 40 min.

"slow responding cell":

A second type of hole-conductor free, high-stability, "slow responding" devices were prepared according to the procedure reported by Anyi Mei et al.[3] Patterned FTO substrates, with blocking layers, were coated with a mesoporous TiO_2 layer (Dyesol 18NRT) diluted with ethanol, screen printed and calcined at 500 °C for 30 min. Once cooled, a 2 micron ZrO_2 over layer was deposited by screen printing, and then carbon electrode, prepared from a dispersion of carbon black and graphite, was deposited and heat treated at 500 °C for 30 min to give an approximate 10 micron rear electrode. The active layer was formed by drop casting a 40 wt% mixed-cation perovskite pre-cursor solution as described by Anyi Mei et al. and further dried at 50 °C for 60 min.

Packaging

The enclosure lid had an aperture cut out that was 2mm larger in each dimension than that of the exposed device area. A piece of *Pilkington* 1.1mm Optiwhite glass was attached using *Sikaflex* 221 sealant as an aperture window on the inside of the lid. Inside the container, a mask defining the area for illumination was screwed in place between the device and the aperture window. A machined aluminium device mount was attached to the bottom of the enclosure, with a thickness chosen to set the height of the device to just below the mask. The mount provided housing for a K-type thermocouple to enable cell temperature measurements (at the rear of the cell). The cell wires were soldered to a *Lemo* four pin socket mounted on the container wall to enable full 4-wire measurements. Next to the socket a cable gland was mounted to provide a seal for the thermocouple cable exiting the container. Inside the container, multiple 0.5 gram indicating desiccant sachets were used to monitor and provide some control over moisture ingress. The lids were affixed to the enclosure bases under nitrogen atmosphere using four corner mounted screws and an edge gasket. Finally the enclosure was spray-painted matte black finish to minimise reflections.

2. Area measurements

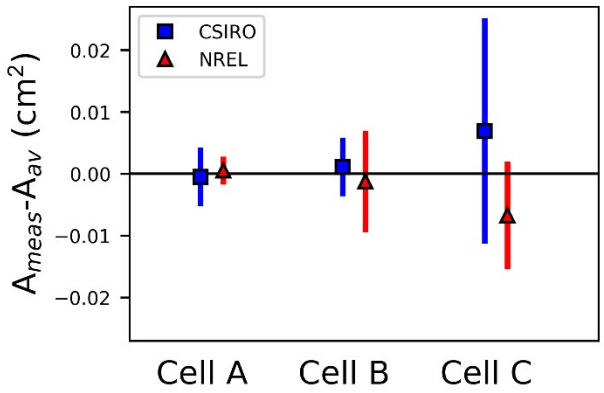

Fig. S1:Comparison of area measurements between CSIRO and NREL for cells A and B (perovskite) and C (silicon). Errorbars indicate the absolute uncertainty for each measurement, expressed to a confidence level of approximately 95%.

Fig. S1 shows the area values measured by CSIRO and NREL for the inter-comparison samples. The plotted quantity is the difference between the measured area (A_{meas}) and the average of the measurements (A_{av}) made by the two laboratories. The values of A_{av} are 1.0315, 1.0221 and 4.177 cm^2 for cells A, B and C, respectively. The measurements are in agreement to within the reported uncertainty

3. EQE measurements

In Fig.s S2-4, the measured external quantum efficiency (EQE) data reported by NREL and CSIRO are presented.

NREL's approach with perovskites is to measure QEs at more than one bias light irradiance. NREL also tests the effect of chopping frequency by adjusting it up and down and watching the response at one wavelength and observing the signal shape on oscilloscope.

The chopping frequencies used at CSIRO for all samples was 120 Hz, and for NREL measurements the frequency was 264 Hz for the perovskite cells the for the silicon cell, which was measured on a different system, the frequency was 100 Hz. Both absolute and relative EQE are presented, although it is the relative quantity that is important for efficiency measurement, as the spectral mismatch factor is sensitive only to the spectral distribution and not the absolute magnitude of EQE. Here, the DC current generated by the cell due to white bias light illumination is used as a proxy for the magnitude of that irradiance.

For cell A, both the absolute and relative EQE are dependent on the bias irradiance. Both CSIRO and NREL observed that the absolute EQE decreased with increasing bias irradiance. The dominant trend in the relative EQE is an increase with bias irradiance for wavelengths above 500 nm and a reduction with bias irradiance for wavelengths below 500 nm. The bias irradiance also strongly influences the absolute EQE, and to a lesser extent, the relative EQE, for cell B. In contrast, the absolute EQE (and therefore also the relative) measured for cell C is relatively invariant as the bias irradiance is changed. The curves used by CSIRO to calculate the spectral mismatch factor were those corresponding to DC currents of 2.8, 0.2 and 4 mA, for cells A, B and C, respectively. For NREL, the irradiance levels for the chosen curves were 4.6 mA, 4.8 and 19.1 mA for cells A, B and C, respectively.

As expected, the relative EQE curves as measured by CSIRO and NREL for cell C are in good agreement. For the perovskite cells however, the agreement is not as strong, in particular for cell A. To estimate how significant the discrepancy in EQE was on the discrepancy in reported I-V results, we use the lamp spectral irradiance and reference cell EQE in place during the CSIRO measurements to calculate the spectral mismatch factors obtained using the CSIRO- and NREL- measured EQEs, respectively. The resulting spectral mismatch factor values differ by 0.1%, and it follows that the short-circuit current density and efficiency would differ by this same relative amount due to the choice of EQE alone. In contrast, the short-circuit current densities reported by both labs differed by significantly more: 11.7 % (where the forward-scan CSIRO measurement made immediately prior to the NREL measurement was compared to value derived from NREL's dynamic I-V measurement). Therefore, there is no evidence that the difference in measured EQE spectra was a significant factor in the discrepancy between the I-V results reported by the two labs.

NREL also reported that, depending on the choice of bias level, the effect on the calculated spectral mismatch factor (for their solar simulator and reference cell) was 0.5% for cell A and 0.06% for cell B.

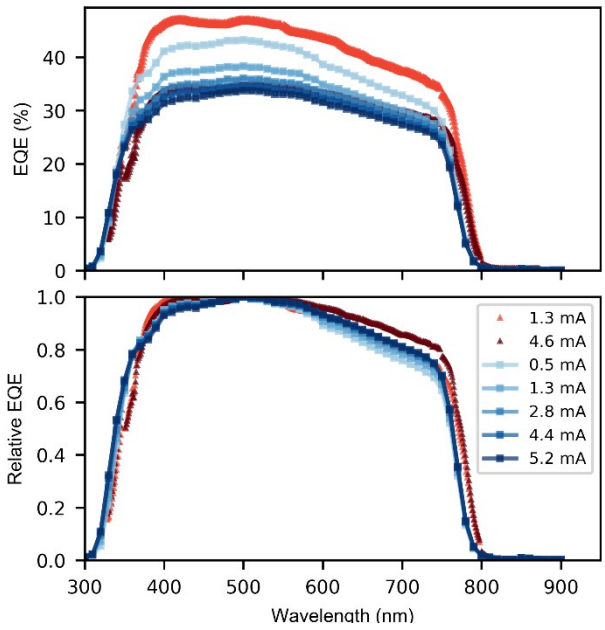

Fig. S2: Measured external quantum efficiency (EQE) at 0 V for cell A ("slow" perovskite) as reported by CSIRO (blue squares) and NREL (red triangles). Darker colours are used to represent larger values of bias irradiance present (quantified using the DC current generated by the cell) during the measurement.

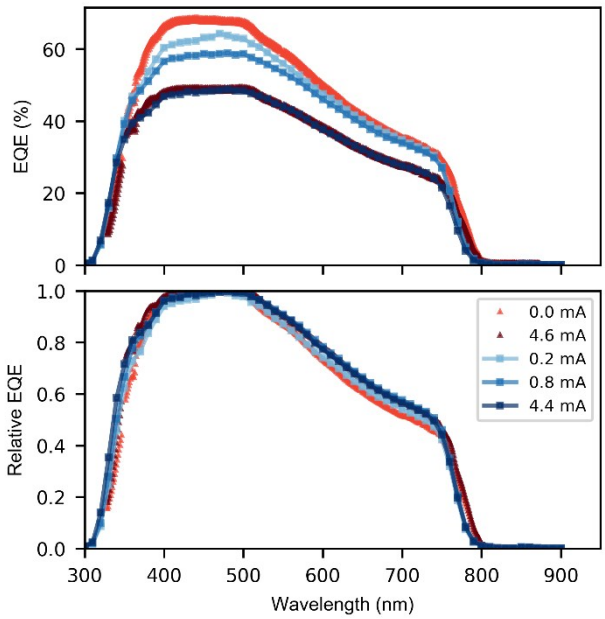

Fig. S3: Measured external quantum efficiency (EQE) at 0 V for cell B ("fast" perovskite) as reported by CSIRO (blue squares) and NREL (red triangles). Darker colours are used to represent larger values of bias irradiance present (quantified using the DC current generated by the cell) during the measurement.

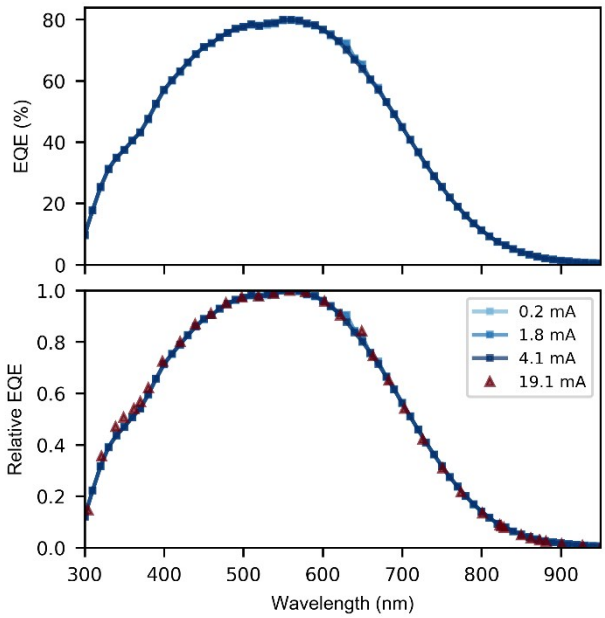

Fig. S4: Measured external quantum efficiency (EQE) at 0 V for cell C (KG1 filtered c:Si) as reported by CSIRO (blue squares) and NREL (red triangles). Darker colours are used to represent larger values of bias irradiance present (quantified using the DC current generated by the cell) during the measurement. For this cell, NREL reported only the relative EQE.

4. Inter-comparison results for cell C

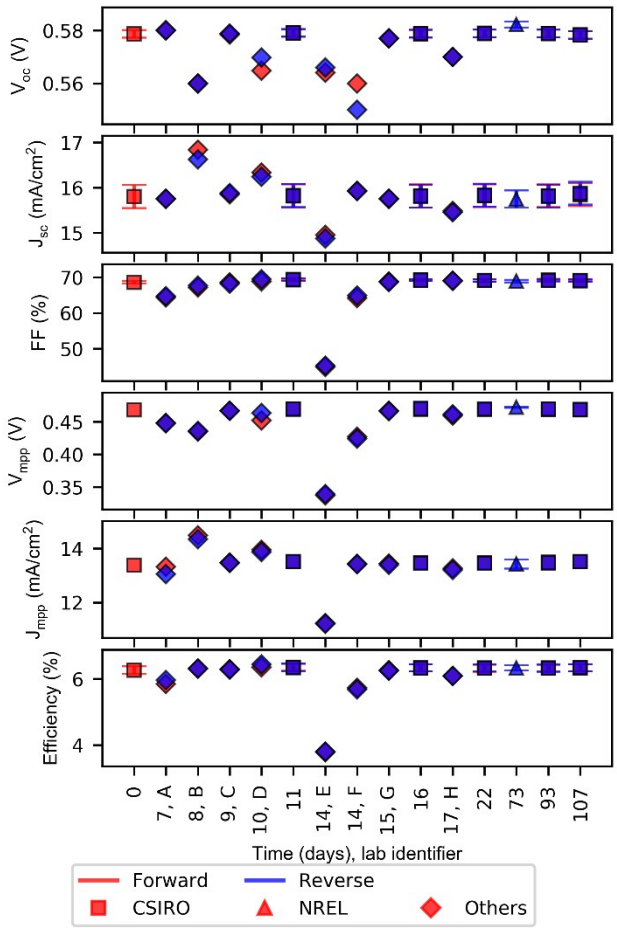

Fig. S5: This Fig. is identical to Fig 1 of the main text, but additionally includes the results for lab E.

5. Measurement sequence for investigation of scan rate dependence of perovskite devices

Below, the sequence of pre-conditioning and measurement used in the investigation is outlined.

Experiment Start

1. Shutter opens. 5 min pre-conditioning at SC under illumination (to allow temperature equilibration and device equilibration under illumination at SC).

I-V Scans (forward and reverse)

2. 5 min pre-conditioning at SC under illumination (to allow device equilibration under illumination at SC)
3. I-V scan in the forward direction.
4. 5 minutes pre-conditioning at near OC under illumination (to allow device equilibration at near OC)
5. I-V scan in the reverse direction
6. Repeat 2-5 with next scan rate.
7. Once all scan rates have been completed, repeat sequence (steps 2-6).

Experiment end

8. Shutter closes. Cell at SC.

The term device equilibrium has been used to denote the equilibration of the devices' collective transient optoelectronic responses to a change in conditions. Following the initial opening of the shutter, steps 1 and 2 provide a total period of 10 minutes of device pre-conditioning to ensure temperature and device equilibration under illumination. Following this, illumination is not interrupted until the end of the experiment to maintain temperature equilibration and to avoid introducing transients due to changes in irradiance.

The resulting I-V curves for cell B are shown in Fig. S6. For cell A, see the main text.

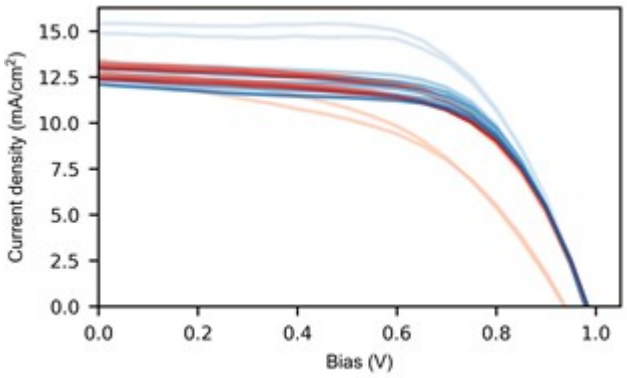

Fig. S6: An investigation of the scan-rate dependence of I-V curves for cell B performed at CSIRO. Forward scans are shown in red and reverse scans in blue. Shading indicates scan speed: light (slow) to dark (fast). The trialled scan speeds are 100, 4.5, 2.3 and 1.3 mV/s

6. Stability of perovskite devices

The perovskite devices were measured a total of seven times by the host laboratory during the inter-comparison. Each time, the same measurement method was used.

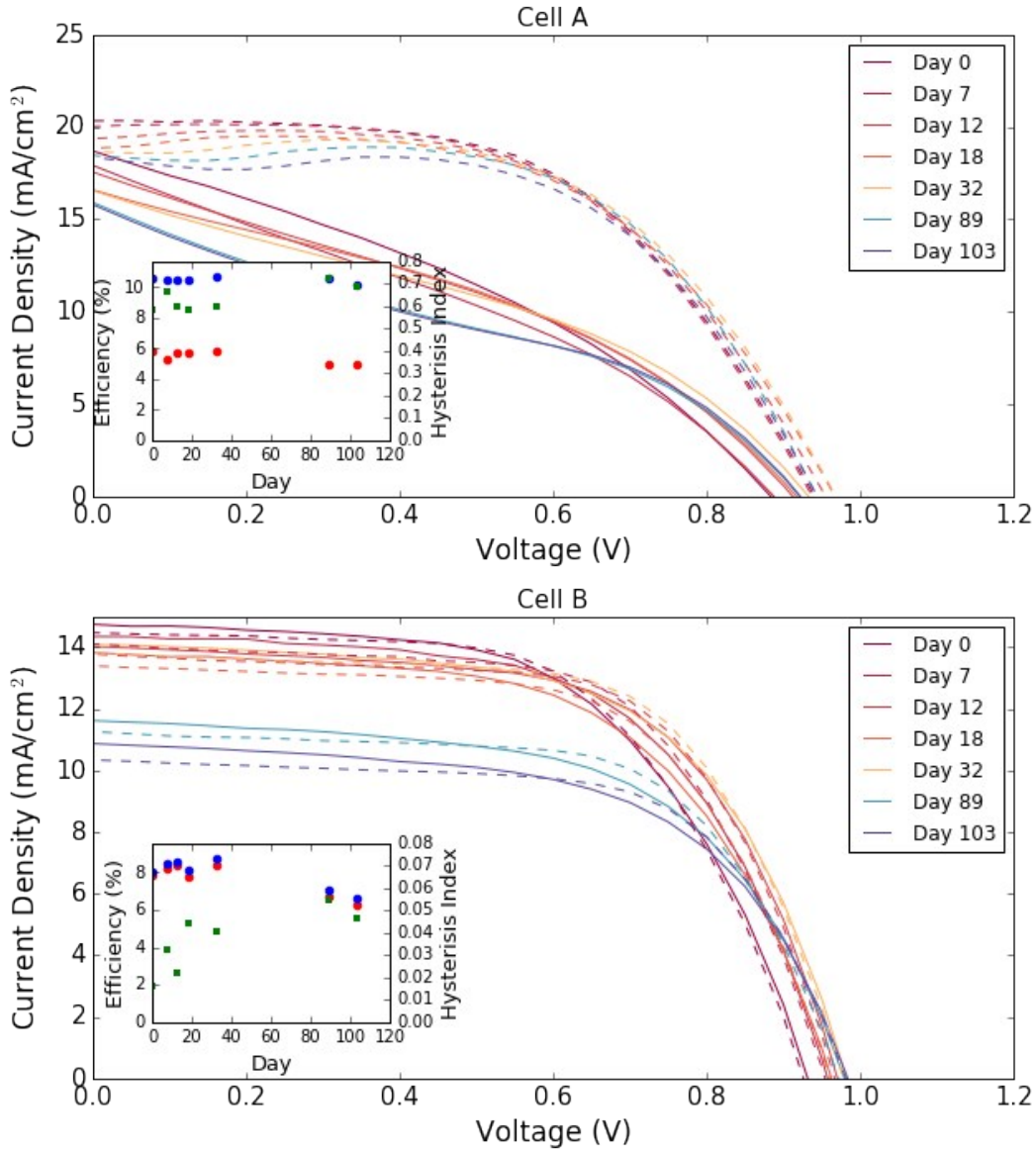

Fig. S7: I-V curves as measured periodically throughout the inter-comparison by the host laboratory using identical measurement procedures. The hysteresis index was calculated according to the form proposed by Levine et al.[4]

7. Influence of technique on measured efficiency: cell B

This plot is the equivalent, for cell B, of Fig. 13 in the main text. Standardised measurements were not performed at CSIRO following the inter-comparison as the device had already exhibited indications of degradation following international transit, hence only the inter-comparison results are shown.

The data in Fig. S8 suggests a strong dependency of reported efficiency on measurement technique. Similar to cell A, the OC soak still clearly over-estimates the efficiency. In contrast, for cell B, the forward measurements using SC soak and the Repeat technique are in good agreement with the Dynamic measurement, and the corresponding reverse measurements over-estimate the efficiency. The Slow technique is in good agreement with the Dynamic value, consistent with the assertion that the scan parameters used for the Slow I-V curves deliver steady-state results (Fig.4 of the main text).

Interestingly, the trend observed in Fig. 13, where the efficiency increases from left to right according to this ordering of techniques, is not evident here. Instead, the reported efficiency is observed to be smallest for the Dynamic method, followed by Slow, SC soak, Repeat and OC soak. This highlights the fact that the role of measurement technique is architecture-dependent.

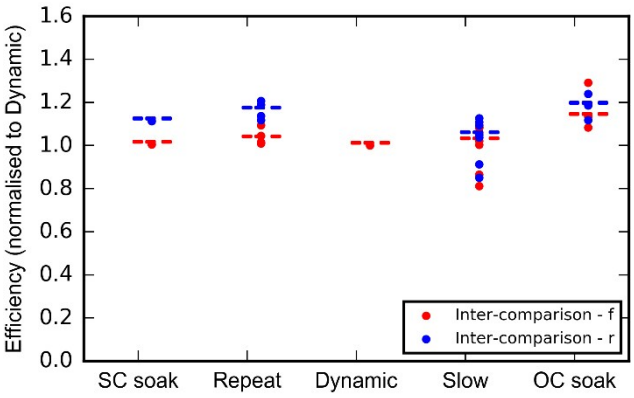

Fig. S8: The reported efficiency of cell B for five trialled I-V measurement techniques. f=forward and r=reverse scan directions. The data is normalised to the Dynamic result. The scan rate for the SC soak, Repeat and OC soak is the same as described in the caption for Fig.10 in the main text. Horizontal lines show the median values for each category.

8. Device efficiency

The loss in device performance introduced by the additional packaging used in the study is assessed here by using a UV-Vis transmission measurement shown in Fig S9. Combining the transmission data with the AM1.5 reference spectrum indicates that the device receives only 91% of the incident irradiance (over the range of active wavelengths). The best estimate of efficiency from the study places Cell A at 8.6% (NREL) and Cell B at 8.4% (PVPL). This means the unpackaged cell efficiency would be 9.4% and 9.2% respectively.

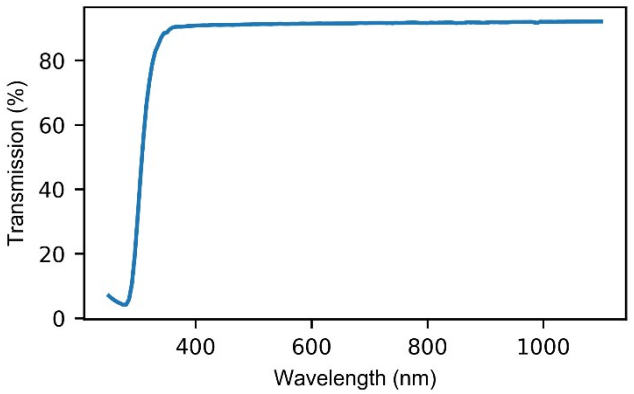

Fig. S9: UV-Vis transmission measurement performed on device packaging window. Over the range of wavelengths of interest for the perovskite device (300 - 850 nm) the transmission is 91%.

References

1 H. Zhou, Y. Shi, Q. Dong, H. Zhang, Y. Xing, K. Wang, Y. Du and T. Ma, *J. Phys. Chem. Lett.*, 2014, **5**, 3241–6.

2 J. Burschka, N. Pellet, S.-J. Moon, R. Humphry-Baker, P. Gao, M. K. Nazeeruddin and M. Grätzel, *Nature*, 2013, **499**, 316.

3 A. Mei, X. Li, L. Liu, Z. Ku, T. Liu, Y. Rong, M. Xu, M. Hu, J. Chen, Y. Yang, M. Grätzel and H. Han, *Sci.* , 2014, **345** , 295–298.

4 I. Levine, P. K. Nayak, J. T. W. Wang, N. Sakai, S. Van Reenen, T. M. Brenner, S. Mukhopadhyay, H. J. Snaith, G. Hodes and D. Cahen, *J. Phys. Chem. C*, 2016, **120**, 16399–16411.